Fracture mechanical analysis of self-fatigue in surface compression strengthened glass plates

M. BAKIOGLU, F. ERDOGAN, D.P.H. HASSELMAN*

Department of Mechanical Engineering and Mechanics and *Ceramics Research Laboratory, Lehigh University, Bethlehem, Pennsylvania, USA

This paper presents a fracture mechanical analysis of the static fatigue and spontaneous fragmentation of surface compression-strengthened glass plates in the absence of applied load. It is suggested that if an initial surface crack which is sufficiently deep to penetrate into the tensile zone within the plate interior is introduced into the plate, then static fatigue, and eventually spontaneous fracture may follow. The crack problem for glass plates under various internal stress fields is solved and the stress intensity factor is obtained as a function of the crack depth. Using the fracture toughness and the slow crack growth characterization of the material, the conditions for no crack propagation, crack propagation leading to crack arrest, and that leading to catastrophic failure are established and discussed. The general results obtained are illustrated by means of a numerical example based on a 2 mm thick surface compression-strengthened glass plate exposed to water at 25° C.

1. Introduction

The strength of brittle materials, particularly their impact and fatigue resistance, can be improved significantly by introducing residual stresses into the medium which are compressive at and near the surface. Such compressive stresses can be created by tempering, ion-exchange, or cladding with another material having a lower coefficient of thermal expansion. Particularly for glasses, strengthening by either tempering or ion-exchange has found wide applications for a large variety of industrial and consumer products. However, glasses strengthened in this fashion appear to be susceptible to spontaneous fragmentation even during the complete absence of applied loads.* A preliminary qualitative consideration of the many factors which could be responsible for this type of spontaneous fracture suggested that it was most likely due to the slow growth of surface cracks which may have been caused, for example, by an incidental impact at some time prior to the frag-

mentation. The driving force for this subcritical crack propagation is provided by the internal stresses. Slow crack growth would be possible if the initial surface crack is sufficiently deep so that the crack tip is in the tensile stress zone in the material interior. The methods of failure prediction for brittle ceramics subjected to stress-corrosive environments are well established and have been applied successfully to the prediction of static fatigue [1], strain-rate sensitivity [2], single-cycle thermal shock [3], as well as thermal fatigue [4, 5]. It should be possible to carry out a similar failure analysis of the static fatigue of strengthened glasses under internal stresses only, provided the proper fracture mechanics analysis is available. The purpose of this paper is to present such an analysis for flat plates under a given state of internal stress in order to establish the quantitative basis for corresponding failure criteria. The analytical results obtained are illustrated by considering a numerical example.

---

*Such a problem was encountered in relation to an eye-lens during a consulting case by one of the authors (DPHH).
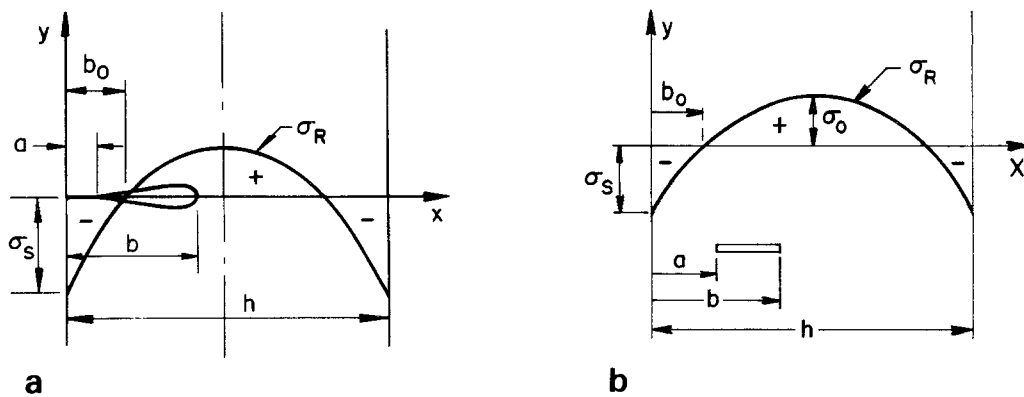
Figure 1 The crack geometry in a plate under residual stress field.

2. Formulation and solution of the crack problem

The two-dimensional problem under consideration is described in Fig. 1. It is assumed that a homogeneous, isotropic, elastic plate of thickness h is under a given state of residual or internal stresses which is compressive near and at the surfaces and tensile in the interior. The plate is otherwise free from the external loads. Thus, the internal stresses are in self-equilibrium and satisfy conditions of the following form:

$$\int_0^h \sigma_R(x)\mathrm{d}x = 0, \qquad \sigma_R(x) = \sigma_{yy}(x, 0). \quad (1)$$

It is assumed that the plate contains an edge crack which is perpendicular to the surface and has a depth b, where $b_0 < b < h$ as shown in Fig. 1a. Because of the compressive stresses near the boundary, the crack faces along $0 \leqslant x < a$ will be closed and will be under compression, the distance a being one of the unknowns in the problem. The crack is open only between $x = a$ and $x = b$, and because of the smooth contact of the crack surfaces, at $x = a$ the "crack tip" is cusp shaped rather than being parabolic. This means that if the problem is treated as a contact-crack problem, at the end point $x = a$, the stress intensity factor k_a must be zero. Thus, the condition

$$k_a = 0 \quad (2)$$

provides the additional information in the solution of the problem to determine the distance a. The problem shown in Fig. 1a is solved for a given distribution of internal stress by considering an arbitrarily located crack along $a < x < b$, ($a > 0$, $b < h$), and for a fixed b, determining the value of

a for which $k_a = 0$. For the solution the standard superposition technique is used, in which the solution of the plate with stress-free crack is assumed to be the sum of two solutions: (1) the plate without the crack having the internal stress $\sigma_{yy}(x, y) = \sigma_R(x)$, and (2) the plate in which the only applied load is the crack surface traction given by

$$\sigma_{yy}(x, 0) = -\sigma_R(x), \qquad a < x < b. \quad (3)$$

To compute the stress intensity factor at the crack tip $x = b$, clearly it is sufficient to consider problem 2 only.

It has been shown that [6–8] the formulation of the general problem (shown in Fig. 1b) leads to the following singular integral equation [8]:

$$\frac{1}{\pi} \int_a^b \left[\frac{1}{t - x} + k(x, t) \right] f(t)\,\mathrm{d}t$$

$$= -\frac{1 + \kappa}{4\mu} \sigma_R(x), \qquad a < x < b \quad (4)$$

where Equation 3 has been used for the crack surface traction, μ is the shear modulus of the material, $\kappa = 3 - 4\nu$ for plane strain and $\kappa = (3 - \nu)/(1 + \nu)$ for plane stress, ν being the Poisson's ratio. In Equation 4 the unknown function is defined by

$$f(x) = \frac{\partial}{\partial x} v(x, 0) \quad (5)$$

where v is the crack surface displacement, and the Fredholm kernel $k(x, t)$ is given by

$$k(x, t) = \int_0^\infty [\kappa_1(x, t, s) - \kappa_1(h - x, h - t, s) + \kappa_2(x, t, s) - \kappa_2(h - x, h - t, s)]\,\mathrm{d}s,$$

1827

$$\kappa_1(x, t, s) = [P(s)\, e^{-s(2h+x+t)}$$
$$- R(s)\, e^{-s(2h+t-x)}]\, /Z(s),$$

$$\kappa_2(x, t, s) = [B(s)P(s)\, e^{-s(2h+x+t)}$$
$$- A(s)R(s)\, e^{-s(2h+t-x)}]\, /Z(s),$$

$$P(s) = e^{2hs} - 1 - 2hs - 2ts(e^{2hs} - 1),$$

$$R(s) = 2hs - 1 + e^{-2hs} - 4ths^2,$$

$$Z(s) = (1 - e^{-2hs})^2 - 4h^2 s^2\, e^{-2hs}$$

$$A(s) = \tfrac{1}{2}\, [1 - 2(h - x)s + e^{2(h-x)s}],$$

$$B(s) = \tfrac{1}{2}\, [1 + 2(h - x)s + e^{-2(h-x)s}]. \quad (6)$$

Solution of Equations 4 and 2 gives the unknown function $f(x)$ and the unknown constant a. After $f(x)$ is determined, the stress intensity factor at the crack tip $x = b$ may be determined from

$$k_b = -\lim_{x \to b} \frac{4\mu\sqrt{\pi}}{1 + \kappa} \sqrt{[2(b - x)]}\, f(x). \quad (7)$$

The integral Equation 4 is solved by using the technique described by Erdogan and Gupta [9].

3. Calculation of crack propagation and failure times

The solution of the crack problem gives the stress intensity factor k_b as a function of b which may be expressed as

$$k_b = F(b). \quad (8)$$

Let K_T be the threshold value of the stress intensity factor for the material, defined as the minimum value required for slow crack growth, and let K_{IC} be the critical stress intensity factor corresponding to catastrophic failure. Also, let the expression

$$\frac{db}{dt} = G(k_b) = G[F(b)] = g(b), \quad (9)$$

giving the slow crack growth velocity as a function of the stress intensity factor or, through Equation 8, as a function of the crack depth, be known. For a given internal stress profile, slow crack growth will occur only when $k_b > K_T$ or

$$[F(b)]_{max} > K_T \quad \text{and} \quad b_i > b_1 \quad (10)$$

where b_i is the initial crack length introduced into the plate at $t = 0$, and b_1 is the minimum crack depth necessary for the initiation of slow crack growth obtained from (see insert in Fig. 7)

$$F(b_1) = K_T, \qquad F'(b_1) > 0. \quad (11)$$

The slow crack growth would be eventually arrested if

$$K_T < [F(b)]_{max} < K_{IC}, \quad b_i > b_1. \quad (12)$$

In this case, from Equation 9 the time to crack arrest may be obtained as

$$T_a = \int_{b_i}^{b_a} \frac{db}{g(b)} \quad (13)$$

where b_a is the second root of Equation 11, i.e. (see Fig. 7)

$$F(b_a) = K_T, \qquad F'(b_a) < 0. \quad (14)$$

On the other hand, if, in addition to the slow crack growth condition 10, the condition

$$[F(b)]_{max} > K_{IC} \quad (15)$$

is satisfied, then the plate may fail catastrophically and the time to failure may be obtained from

$$T_f = \int_{b_i}^{b_2} \frac{db}{g(b)} \quad (16)$$

where the critical crack length b_2 is obtained from (see Fig. 7)

$$F(b_2) = K_{IC}, \qquad F'(b_2) > 0. \quad (17)$$

Here, it is assumed that when $k_b = K_{IC}$ the fast fracture would begin, and since subsequently $k_b > K_{IC}$ for some small period of time (see Figs. 2 to 4) the crack would further accelerate. Then because of the dynamic effects, it may be conjectured that the crack would propagate through the entire plate thickness even if the crack driving force or k_b eventually falls below K_{IC} when the crack approaches the opposite surface. However, if $(k_b)_{max}$ is not much greater than K_{IC}, the dynamic effects may not be sufficient to cause the crack to penetrate through the entire plate thickness.

4. Numerical example and results

Stress intensity factors were generated for three selected symmetric residual or internal stress fields expressed by

$$\sigma_R^1(x) = \sigma_0\, [1 - 3(2x/h - 1)^2], \quad (18)$$

$$\sigma_R^2(x) = \sigma_0\, [1 - 5(2x/h - 1)^4], \quad (19)$$

$$\sigma_R^3(x) = \sigma_0\, [1 - 7(2x/h - 1)^6] \quad (20)$$

where σ_0 is the tensile stress at the midplane of the plate (Fig. 1). Parabolic stress distribution (Equation 18) is typical for a tempered glass,
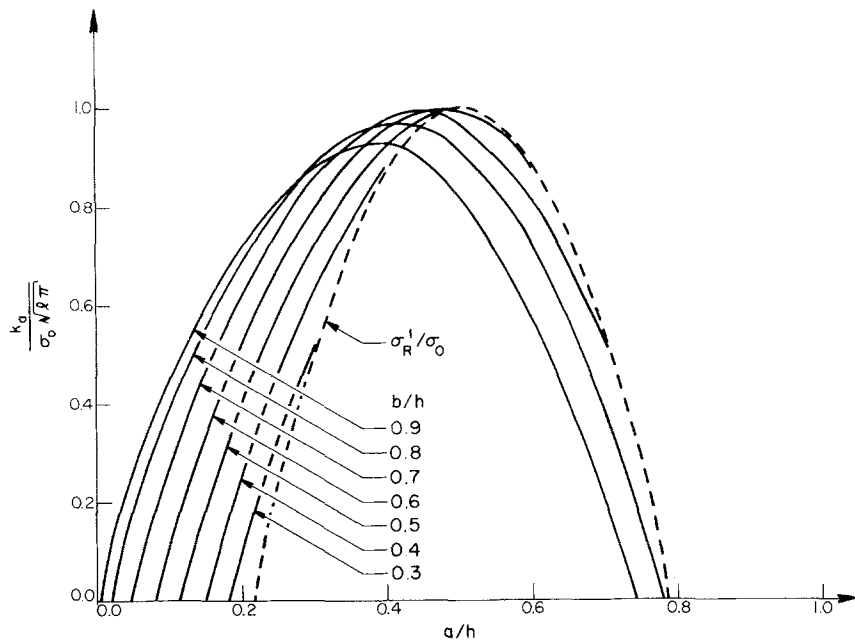
Figure 2 Stress intensity factor at the left end of the crack, k_a, for arbitrary crack size and orientation in a plate in which the residual stress is a second degree polynomial.
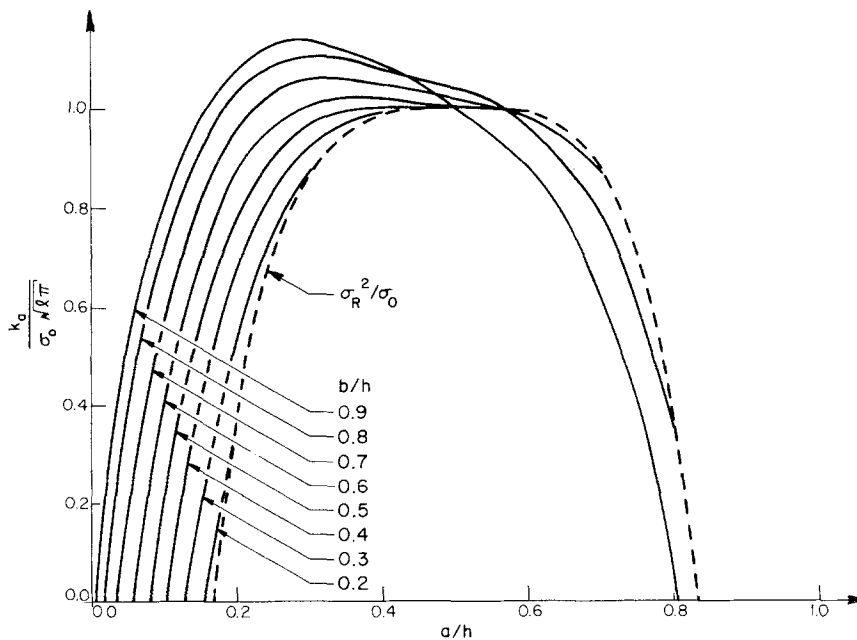

Figure 3 Stress intensity factor k_a in a plate where the residual stress is a fourth degree polynomial.

whereas the 6th degree polynomial distribution (Equation 20) may be more representative of a glass strengthened by ion exchange. Figs. 2 to 4 show the stress intensity factor k_a at the crack tip $x = a$ for any given values of a and b (Fig. 1b). In these figures k_a is normalized with respect to $\sigma_0\sqrt{(\pi l)}$, where $l = (b - a)/2$. Since the loading is symmetrical, corresponding k_b values may be obtained by considering mirror images of the crack with respect to the mid-plane. The figures also show the tensile part of the internal stresses given by Equations 18 to 20. From these figures it may
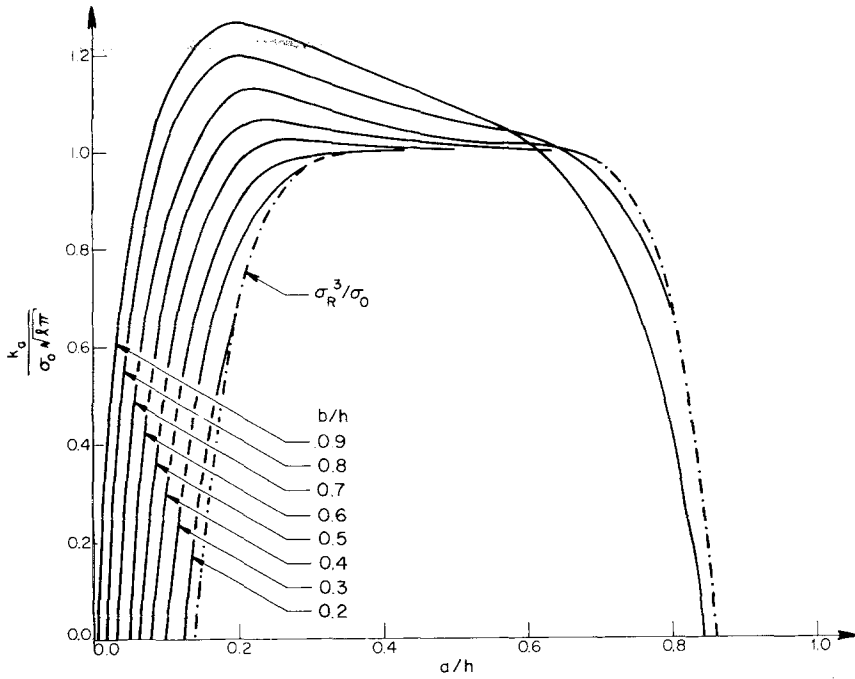
1829

Figure 4 Stress intensity factor k_a in a plate where the residual stress is a sixth degree polynomial.
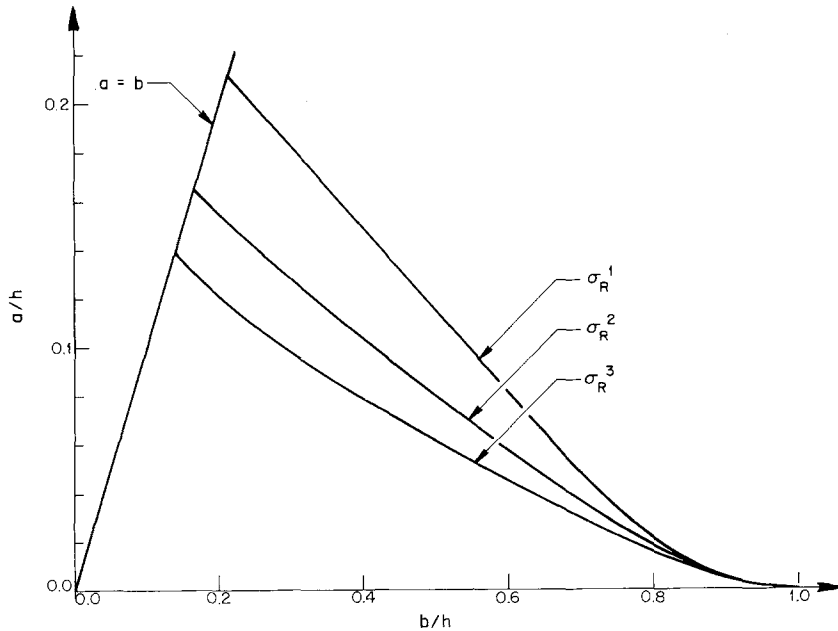

Figure 5 The value of the crack closure distance a (corresponding $k_a = 0$) as a function of the crack depth b.

be observed that

$$\frac{k_a}{\sigma_0 \sqrt{(\pi l)}} \rightarrow \frac{\sigma_R}{\sigma_0} \quad \text{as } b \rightarrow a \qquad (21)$$

which is expected, since when $b \rightarrow a$, the crack length $2l$ is very small compared to a and b, and

essentially the problem becomes one of an infinite plane containing a crack of length $2l$ subjected to uniform pressure σ_R for which $k_a = \sigma_R \sqrt{(\pi l)}$.

Fig. 5 shows the crack closure distance a corresponding to $k_a = 0$ for the three internal
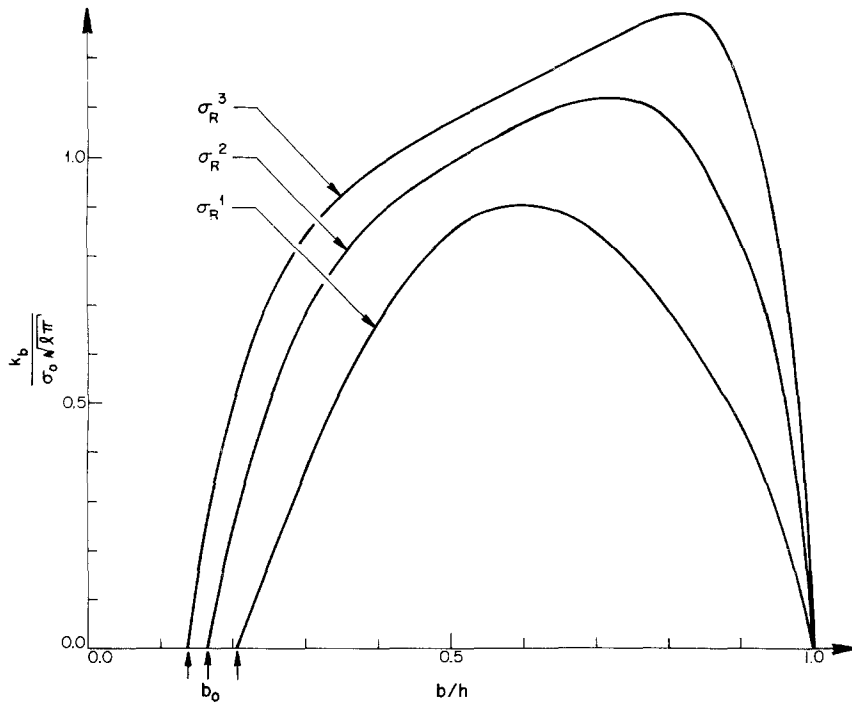
1830

Figure 6 The stress intensity factor k_b (corresponding $k_a = 0$) for the three residual stress fields.

stress distributions (Equations 18 to 20) (see Fig. 1a). In Fig. 5 the intersection of the $a = b$ line with the a versus b curve corresponds to the point $x = b$ at which the internal stress is zero. Thus, note that a is always less than b_0 and $a \to b_0$ when $b \to b_0$.

From the viewpoint of static fatigue analysis, the most relevant information is the stress intensity factor k_b obtained as a function of b, for which $k_a = 0$ (i.e. Equation 8). For the three internal stress profiles (Equations 18 to 20) these functions are shown in Fig. 6. In this figure too, k_b is normalized with respect to $\sigma_0 \sqrt{(l\pi)}$, $l = (b - a)/2$. Therefore, before using it in, for example, Equations 9, 13 or 16, a and l should be expressed in terms of b through the results given in Fig. 5.

For a numerical example, the analytical results presented above were applied to a 2 mm thick soda lime-glass plate with an internal stress distribution given by Equations 18 or 20, exposed to a water environment at $25°C$. As measured by Wiederhorn and Bolz [10], the rate of slow crack growth may be expressed as:

$$(\mathrm{d}b/\mathrm{d}t) = V_0 \exp\left[(ck_b - E)/RT\right] \quad (22)$$

where v_0 and c are constants, and the activation

energy $E = 1.088 \times 10^5$ J mol^{-1}, the gas constant $R = 8.32$ J mol^{-1} $°C^{-1}$ and the temperature $T = 298$ K for the present study. As shown in a previous study [8] devoted to the thermal fatigue resistance of this soda-lime-glass, the rate of slow crack growth most accurately can be described by two bi-linear regions between a fatigue limit, $K_T \approx 2.49 \times 10^5$ N m$^{-3/2}$ and the critical stress intensity factor, $K_{IC} = 7.49 \times 10^5$ N m$^{-3/2}$. For these two bi-linear regions V_0 and C are [8]:

$$\ln V_0 = -1.08, C = 1.088 \text{ for}$$
$$k_b < 3.62 \times 10^5 \text{ N m}^{-3/2}$$

$$\ln V_0 = 10.3, C = 0.110 \text{ for}$$
$$k_b > 3.62 \times 10^5 \text{ N m}^{-3/2}$$

For an optical borosilicate glass exposed to moist air, the crack-growth behaviour is almost identical to the bilinear crack-growth behaviour chosen for the present example. Accordingly, the results obtained are not limited only to the specific glass chosen for the present example.

The results for a parabolic internal stress distribution (Equation 18) are shown in Fig. 7 where the initial crack depth $b_i = b_1$ is just sufficient to start the slow crack growth (see Equation 11). When the magnitude of the compressive sur-
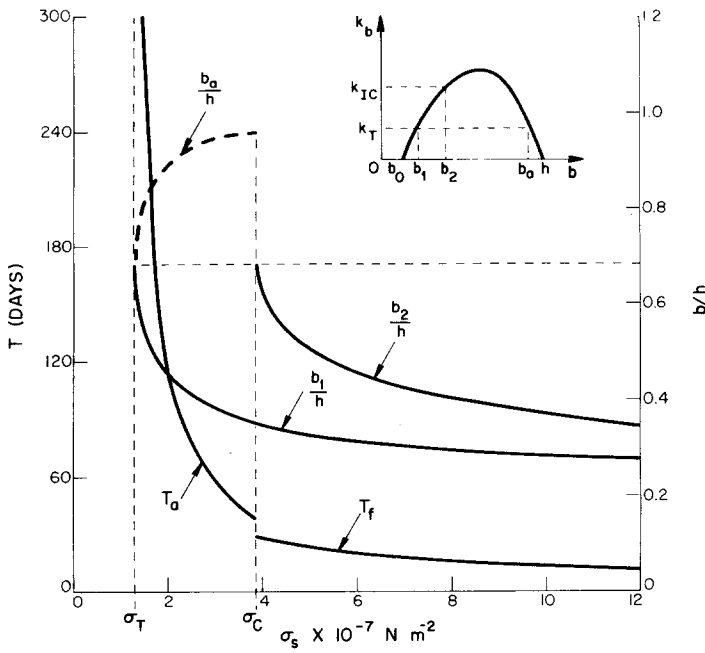
Figure 8 Time-to-failure $T_f(\sigma_s > \overline{\sigma_c})$ and time-to-crack arrest $T_a(\sigma_T < \sigma_s < \sigma_c)$ in a 2 mm thick soda-lime-glass plate in water for $b_i = b_1$. Assumed internal stress field: sixth degree polynomial.
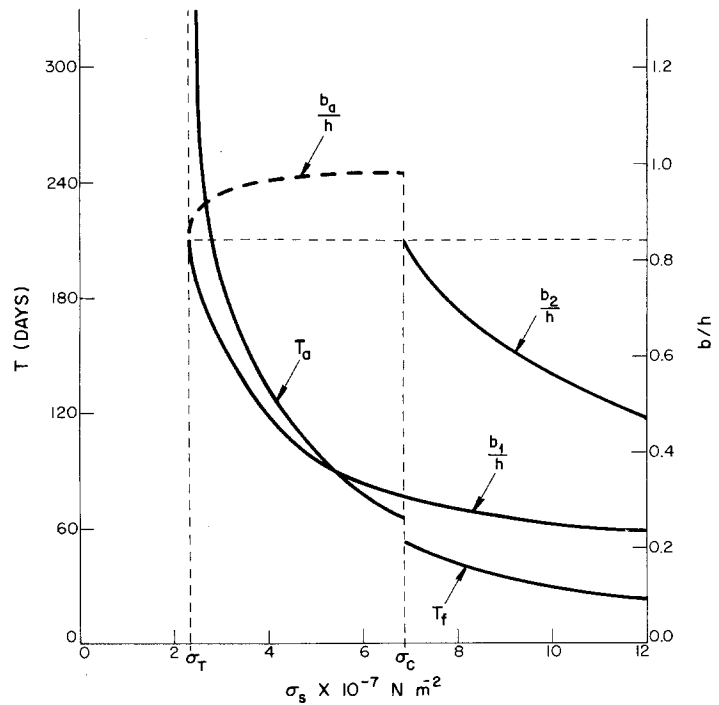
face stress σ_s is greater than a critical stress σ_c, then condition 15 is satisfied and time to failure T_f shown in the figure is calculated from Equation 16. The stress $\sigma_s = \sigma_c$ corresponds to $(k_b)_{max} = K_{IC}$. The figure also shows the critical crack growth length b_2. Note that for greater values of σ_s, smaller values of $b_i = b_1$ are needed to initiate the slow crack growth and shorter time

T_f elapses until catastrophic failure. When σ_s is less than σ_c but greater than a threshold stress σ_T corresponding to $(k_b)_{max} = K_T$, then condition 12 is satisfied and the time for crack arrest T_a shown in the figure is calculated from Equation 13. The discontinuity in the time curve at $\sigma_s = \sigma_c$ is due to the fact that the subcritical crack propagation when $\sigma_s < \sigma_c$ takes place for the increasing
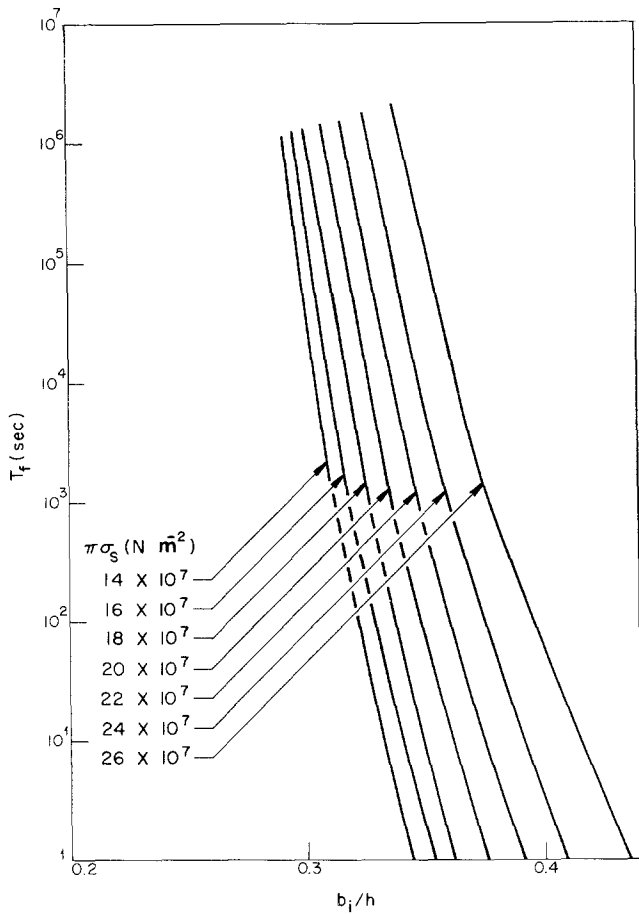
T_f (sec)

$\pi\sigma_s$ (N $\bar{m}^2$)

14 × 10^7
16 × 10^7
18 × 10^7
20 × 10^7
22 × 10^7
24 × 10^7
26 × 10^7

b_i/h

as well as the decreasing branch of the k_b curve, whereas when $\sigma_s > \sigma_c$ it takes place only for the increasing branch (see Equations 13 and 16 and the definitions given by Equations 11, 14 and 17). For $\sigma_T < \sigma_s < \sigma_c$ the arrest value of the crack depth b_a defined by Equation 14 is also shown in the figure. It is seen that when $\sigma_s \to \sigma_T$ (or as $(k_b)_{max} \to K_T$) $k_b = K_T$ line becomes tangent to k_b versus b curve and $b_a \to b_1$. However, for this limiting case, since the crack growth velocity approaches zero, as seen from the figure, T_a asymptotically goes to infinity.

Similar results for an internal stress field given by a sixth degree polynomial (Equation 20) are shown in Fig. 8.

In the results shown in Figs. 7 and 8 it is assumed that $b_1 = b_i$. In a plate with a parabolic internal stress distribution, the time to failure, T_f is shown in Fig. 9 as a function of an arbitrary initial crack length b_i, $(b_i > b_1)$ for various values of σ_s where $\sigma_s > \sigma_c$. Since the surface stress levels shown in Figs. 7 to 9 are within the range of those

encountered in surface compression strengthened glasses, the conclusions that can be drawn from these results is that fracture by static fatigue due to internal stresses only, indeed appears to be possible.

5. Discussion

From the analysis given in this paper, a number of general conclusions may be drawn. Most importantly, the solution indicates that spontaneous fragmentation resulting from static fatigue is indeed a possible mode of failure in surface compression strengthened glasses. In fact, as shown by the numerical example, for high values of internal stress level and initial crack depth, the failure times can be rather short.

Although the increased impact resistance of surface-compression strenghtened glasses must be considered a major advantage, the static fatigue of such glasses which may have received a major damage just short of catastrophic failure during an impact represents a definite hazard. This is

particularly so, since in glasses flaws of sufficient size to cause such failure are very difficult to detect. Clearly, the development of a reliable non-destructive flaw-detection technique in glasses is highly desirable. Even if the crack never became critical and propagated in a slow manner only, the remaining ligament on crack arrest could be only a small fraction of the plate thickness. This would weaken the plate to such an extent that only a small applied load would be required for total failure, again giving rise to a hazardous condition.

To minimize the incidence of static fatigue, clearly it will be advantageous to select or develop glasses with values of K_T and K_{IC} as high as possible, in combination with low rates of crack growth characteristics even in highly stress-corrosive environments. Although the numerical example was carried out for a plate of 2 mm thickness only, the analytical results indicate that for a given internal stress distribution, the static fatigue depends on the ratio of flaw depth to plate thickness. Obviously, then, static fatigue may be reduced even further, or perhaps even eliminated by increasing the total plate thickness.

For an internal stress distribution given by the sixth degree polynomial (Equation 20), for a given value of surface stress the thickness of the compressive zone and the magnitude of the tensile stresses in the interior are expected to be smaller than for a parabolic internal stress distribution. This suggests that for the sixth degree internal stress distribution a shallower initial crack will be required for the static fatigue process than for the parabolic stress distribution. On the other hand, it is also clear that for the sixth degree poly-

nomial, because of the lower tensile stress in the plate interior, the subcritical crack growth velocity will be smaller, the critical crack length will be greater, and consequently time to failure will be longer than for the parabolic stress distribution. These conclusions may be clearly observed by comparing the results given in Figs. 7 and 8.

Acknowledgement

References

1. A. G. EVANS, *J. Mater. Sci.* 7 (1972) 1137.
2. Idem, *Inst. J. Fracture* 10 (1974) 251.
3. R. BADALIANCE, D.A. KROHN and D. P. H. HASSELMAN, *J. Amer. Ceram. Soc.* 57 (1974) 432.
4. D. P. H. HASSELMAN, R. BADALIANCE, and C.H. KIM *J. Mater. Sci.* 11 (1976) 458.
5. D. P. H. HASSELMAN, E. P. CHEN, E. L. AMMAn, J. E. DOHERTY and C. G. NESSLER, *J. Amer. Ceram. Soc.* 58 (11–12) (1975) 513.
6. G. D. GUPTA and F. ERDOGAN, *J. Appl. Mech. Trans. ASME* 41 (1974) 1001.
7. S. KRENK and M. BAKIOGLU, *Int. J. Fracture* 11 (1975) 441.
8. S. KRENK, *Int. J. Solids, Structures* 11 (1975) 693.
9. F. ERDOGAN and G. D. GUPTA, *Q. Appl. Math.* 30 (1972) 525.
10. S. M. WIEDERHORN and L. H. BOLZ, *J. Amer. Ceram. Soc.* 53 (1970) 543.